ISSN 2303-4521
Periodicals of Engineering and Natural Sciences *Original Research*
Vol. 11, No. 2, April 2023, pp.248-261

Experimental investigation and statistical modelling for assessing the sliding wear of Futilized Filament Fabrication (FFF) fabricated parts

Hind B. Ali[1], Haider Basil Ali[1], Mukhallad H. Shawish [1], Saad K. Hasan[1]
[1] Materials Engineering Department, University of Technology -Iraq

ABSTRACT

A significant historical enabler for the improvement of industrial goods has been the characterization of novel materials. For example, a large variety of polymeric materials are readily accessible to manufacture the appropriate items depending on the production method. Due to its capacity to produce components with complicated geometries without the need for tools or a human interface, fused filament fabrication (FFF) is acquiring a unique edge in the industrial sector. By adjusting process parameters at the right values, the qualities of FFF-built items may be enhanced since they rely heavily on these factors. Increasing the service life of functioning components requires taking wear resistance into account. Because of this, the current work concentrates on a thorough investigation to comprehend the impact of 3 crucial elements, including layer thickness, printing speed, also infill density, infill density, and the sliding wear of test specimens. A mechanism of wear is explained by utilizing microphotographs.

Keywords: fused filament fabrication (FFF), sliding wear, ABS, layer's thickness, printing speed, and infill density.

Corresponding Author:

Hind B. Ali
Materials Engineering Department
University of Technology-Iraq
Bagdad - Iraq
E-mail: 130047@uotechnology.edu.iq

1. Introduction

Using a basic software program also polymeric materials with appropriate mechanical and thermal characteristics, Any object, from a basic to very complex shape, has been constructed utilizing fused filament fabrication (FFF) technology. Since this technique can rapidly produce complex structures, It has sparked considerable interest in both the academic and corporate realms. Moreover, it has become common in small-scale industrial settings. [1]. Studies on the qualities of materials made utilizing FFF have increased recently, especially those pertaining to their wear resistance, which is important when a 3D-printed material must slide over the surface of another material while being utilized [2]. ABS 3-Dimensional Printing requires polymers to be as flexible and as mechanically strong as is reasonably conceivable while yet having sufficient stickiness. The fused filament fabrication (FFF) method is an example of an additive manufacturing approach. It is a kind of additive manufacturing, like stereolithography and selective laser sintering, to mention just a few of the other processes that fall into this category. Each FFF technique makes it possible to create a virtual solid model by first slicing the model data into a number of cross-sections in two dimensions (2D). Subsequently, by feeding this fragmented information into an additive manufacturing (AM) machine, it is possible to create the actual physical component. stacked on top of one another [3]. The FFF method is a melt extrusion additive manufacturing (AM) approach in which the heated extruder melts the filament. This is because the temperature of the extruder is always adjusted above the melting point of the polymer that is utilised, and this adjustment is dependent on the viscosity of the polymer. The printing head assembly of a 3D printer may be moved around on a platform thanks to stepper motors (Figure 1). After being compressed and pushed through the extruder, the molten polymer is expelled from the nozzle and onto the platform that is located in the XY plane. After a cross-deposition segment has been successfully completed, the platform or the 3D printing head will accurately shift

one layer's thickness in the Z direction.. [4]. The 3-dimensional (3D) structure is built in line with this concept layer by layer. Up until the component is built, this process is repeated. The solidification time in the FFF process controls the melting mechanism [5].

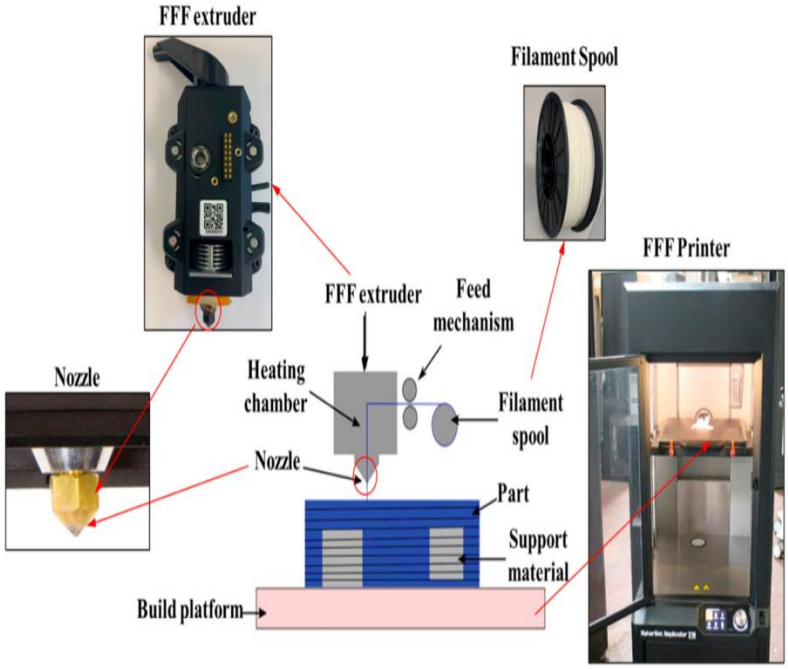

Figure 1. The diagram illustration of FFF process [3]

Following these stages, the Fused Deposition Modelling (FDM) operation procedure is carried out. [6]:
The design or pattern for the required item is created utilizing computer-aided design (CAD) software. The CAD file is loaded by the 3D printer's software. The stereo lithography (STL) file format is used to save all printer and trial settings, as well as the design. The SLT file is loaded into the 3D printing machine, and layer-by-layer manufacturing begins. The polymeric material is extruded in order to carry out the printing. In fact, the heated nozzle of the 3D printer is where the thermoplastic polymer passes before it reaches the heated platform or bed. After the trial is over, the item may be taken out and polished, for example, to enhance its appearance. La Kamaljit and (2016)[7] Under dry sliding circumstances, We investigated and compared the wear parameters of fused deposition modeling (FDM) components made from composite material and ABS feedstock filament.. The tests were carried out for five and ten minutes at room temperature with weights of five, ten, fifteen, and twenty Newtons at a sliding velocity of sixty-three millimeters per second. Both the applied load and the time length had an effect on the amount of wear that occurred, as well as the friction force, the friction coefficient, and the temperature. Priyank (2018) [8] The effect that many aspects of the FDM manufacturing process have on compressive strength was studied. These aspects included layer's thickness, filling, pattern, number of shells, and infill density. A Taguchi orthogonal array served as the basis for the experimental study's design (L8). We conducted two DOEs, each with a different kind of material and equipment, in order to establish which combination of process parameter variables produced the greatest results. PLA and PETG were utilized, respectively, in the Makerbot Replicator 2X and Open Edge HDE machines throughout the printing process, which resulted in the creation of the specimens. The following criteria make up the ideal combination, as determined by the findings of the ANOVA and the S/N ratio: a layer's thickness of 0.2 millimeters, a number of shells equal to four, a diamond infill pattern, and an infill percentage of seventy percent. It was determined that the percentage of infill was the parameter that was the most useful. Keshavamurthy et la. (2020) [9] The goal of this inquiry was to produce results, therefore that's what it accomplished. The purpose of this study is to examine and explain the friction & wear behavior of copper-filled Acrylonitrile Butadiene Styrene (ABS) composites using a method called fused deposition modeling. The fused deposition modeling approach will be used to achieve this (FDM). The filament used in the manufacture of the copper-ABS composite was successfully removed using a procedure known as twin screw extrusion. The friction & wear properties of ABS and ABS-copper composites were investigated under a range of loads and sliding velocities. The weights ranged from very light to very heavy. Copper powder has been included into the composites, which has led to a significant improvement in both the friction & wear properties of the materials. Materials and Fabrication.

2. Methods

The materials employed in the FFF approach are separated between regularly utilized materials, such as polymers and composites (including nanocomposites), and "sustainable materials," a term coined by the authors and comprised of natural and recycled substances [10, 11]. ABS is a 3D printing material for FFF (also known as FDM) technology. ABS is a thermoplastic amorphous polymer manufactured from petroleum. It is not biodegradable and is extruded at high temperatures (between 220 and 280 degrees Celsius). Due of its impact resistance and durability, ABS is extensively utilized in industry, such as for prototyping, toy manufacture, and components for boats and automobiles [12].

Table 1 . ABS mechanical characteristics [13]

Elongation at Break	10 -50%
Elongation at Yield	1.7 - 6 %
Flexibility (Flexural Modulus)	1.6 - 2.4 GPa
Hardness Shore D	100
Strength at Break (Tensile)	22.1 - 74 MPa
Strength at Yield (Tensile)	13 – 65 MPa
Toughness (Notched-Izod Impact at Room Temperature)	8 - 48 KJ/m2
Durability at Low Temperatures (Notched-Izod Impact at Low Temperature)	7 - 22 KJ/m2
Young's Modulus	1.79- 3.2 GPa

A variety of process parameters and their levels were employed to explore and assess process performance. They are the mm/h of printing (50, 75, and 100), the layer's height (0.15, 0.25, and 0.35 mm), and the infill density (0.1, 0.2, and 0.3 mm) (30, 60, and 90 percent). The Futilized Deposition Modelling was utilized to manufacture 9 specimens based on Taguchi method L9 according to design of experiment with suitable dimensions for the required tests. The specimens were designed with UG NX software and then sliced utilizing Cura software, the process parameters must be specified. Specimens were tested for wear resistance. The printing machine that utilized for the fabricated specimens is known as Ultimaker 2+. It supports a wide range of materials, the material that utilized in this work is ABS. The first stage in the work plan of the experimental work was executed according to the work illustrated in Fig. 2

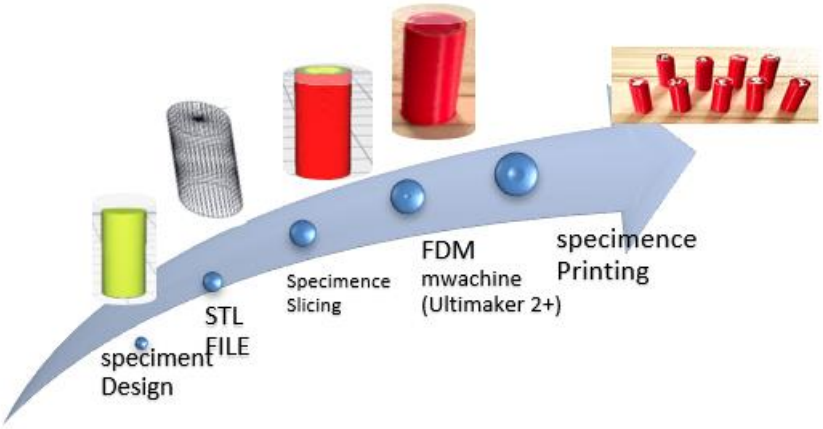

Figure 2. The First Step in Work Plan of Experimental Work

2.1. Specimens Design/ CAD Modelling and UG NX Software

Standard specifications for wear testing were used in the creation of specimens in the CAD application Unigraphics NX, which was then saved as an STL file. One of the forms STL's many uses is that it is supported by computer-aided design software [14] Figure 3 depicts the size (in millimeters) of the standard test samples that must be modeled in accordance with specified criteria. [15] Utilizing Cura, a slicing program, an STL file is exported and opened. In order to achieve this, the slicing program will divide the specimen into the specified

number of thin slices. The process parameters can be set in the slicing program. This program transmits the code to the printer and controls the temperature of the extruder's nozzle. [16].

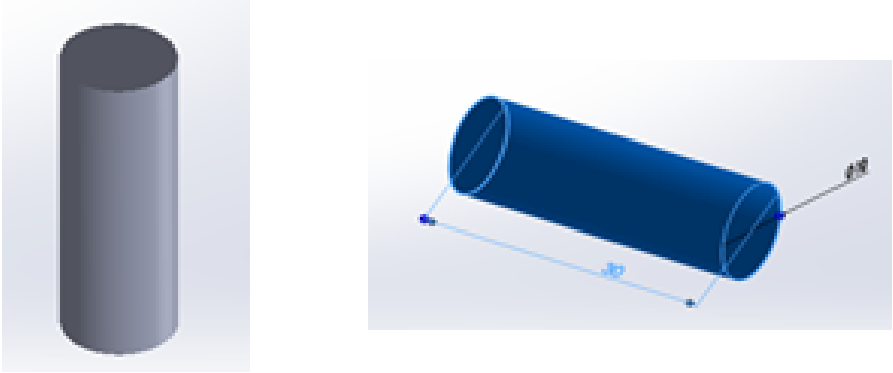

Figure 3. Schematic of Testing Specimen

2.2. Parameter of FFF

Layer's height, or the height of the extruded filaments, is shown in Figure 4 to be the determining factor in how far up the vertical axis a new layer must be added. The layer's height is a crucial parameter in printing; decreasing the layer's height would result in denser voids[17]. As a cost, decreasing the layer's height increases the printing time. In this investigation, the following layer's thicknesses were used: (0.15, 0.25 and 0.35 mm).

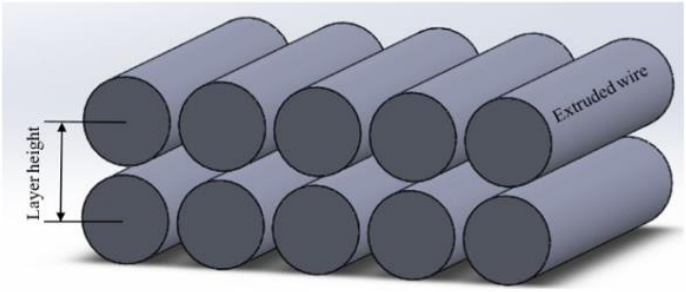

Figure 4. Deposited filaments

fill density: As illustrated in Figure 5, this parameter influences the distance between the lines of the interior filling, which in turn defines the inner piece's solidity percentage. This parameter's percentages may have a considerable effect on the mechanical quality of the components and are crucial in determining overall material usage and cost. [18].

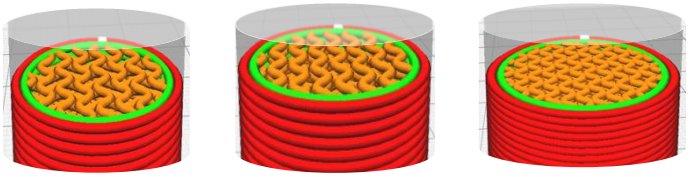

30% 60% 90%

Figure 5. Filling percentages

Infill pattern: In this case, the infill pattern used was gyroid. The gyroid infill is the most interesting design element. Mathematics curves that are computed again and over again are used in an erratic layering pattern. The power of the design comes from the three-level overlap of the curves [19].

Figure 6. Gyroidal forms within the sample

Print speed: An extruder head's linear speed aside it moves across the build platform's XY plane is determined by the printing speed. [20] While changing the printing speed may change the extruded wire's width or diameter, it might be fascinating to investigate how this can affect the mechanical characteristics of the printed objects [21]. This work has employed 3 levels: 50, 75, and 100 mm/s.

2.3. Design of experiments

In the current work, the objective is to investigate the influence of parameters of printing which are (layer's thicknesses, printing speed, infill pattern) on the wear resistance of the parts. These parameters have a major effect on the wear resistance of the model [22]. So, these parameters are chosen for the current work. The range of process parameters and their levels are summarized in Table 2.

Table 2. Main factors and their respective significance

Fixed Factors			Control Factors				
Factors	Amount	Unit	Factors	Levels			Unit
				1	2	3	
Infill Pattern	gyroid	-	Printing velocity	50	75	100	mm/s
Shell thickness	0.2	mm	Layer's thickness	0.15	0.25	0.35	mm
part Orientation	0	degree	Filling density	30	60	90	%
Size of the Nozzle's Diameter	0.6	mm					
printing temperature	200	℃					
levels of Build plate temperature	60	℃					

When utilizing the Taguchi design, it is imperative that an orthogonal array be selected. This investigation considers not just the interplay of orientation with the other aspects, but also three distinct elements at three distinct levels. [23] It is clear that L9 is the appropriate orthogonal array here. A total of 9 different "trial" or "experiment" conditions can be entered across the rows of this array, and each variable or interaction can be assigned in the columns. In order to minimize erroneous analysis, inaccurate results, and to reduce the confounding influence of factors and interactions, variables and their interactions have been allocated according to Table 3.

Table 3. DOE Utilizing Taguchi Method based on Orthogonal Array L9

Sample no.	Printing velocity mm/s	layer's thickness mm	Filling density %
1	50	0.25	30
2	50	0.35	60
3	50	0.15	90
4	75	0.25	60
5	75	0.35	90
6	75	0.15	30

Sample no.	Printing velocity mm/s	layer's thickness mm	Filling density %
7	100	0.25	90
8	100	0.35	30
9	100	0.15	60

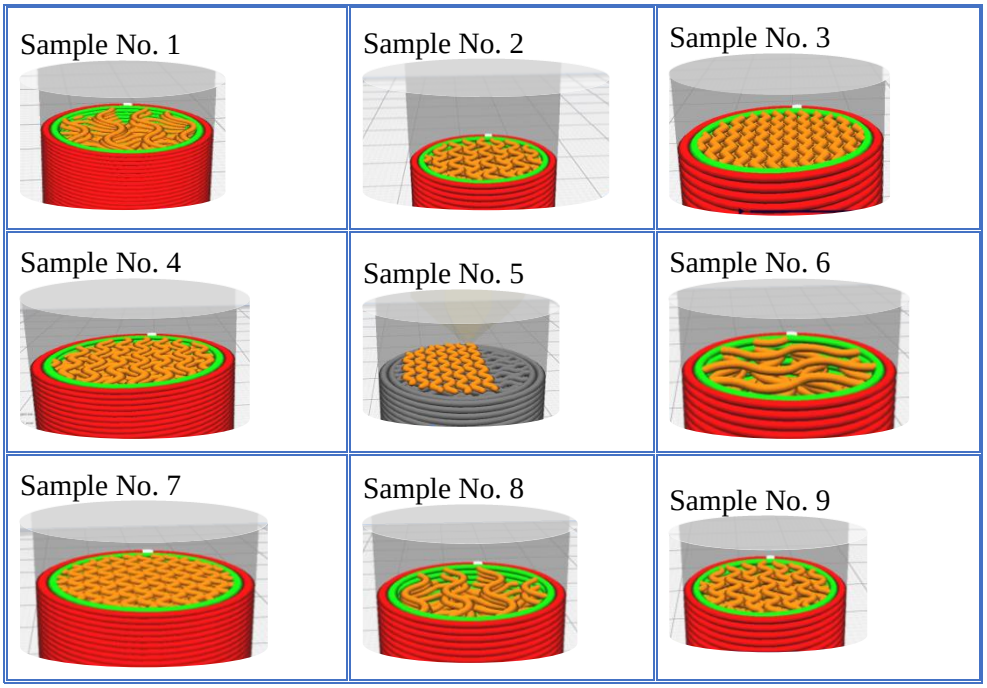

Figure 7. Samples based on Orthogonal Array L9

2.4. Wear testing

Following specimen printing, the wear resistance would be evaluated, and the printing time would be recorded [24]. A sliding wear test was carried out utilizing pin-on-disk equipment in accordance with ASTM G99-04, the Standard Test Procedure for Wear Testing with Pin-on-Disk Equipment. The test was conducted in accordance with the requirements. The findings of this test (Ducom, TR-20LE-M5) are shown in Figure 3. Figure 8 depicts a typical wear testing specimen. It is perpendicular to the circular disc that is flat, and the end contact shape of this component is flat (EN 31 hardened steel) [25].

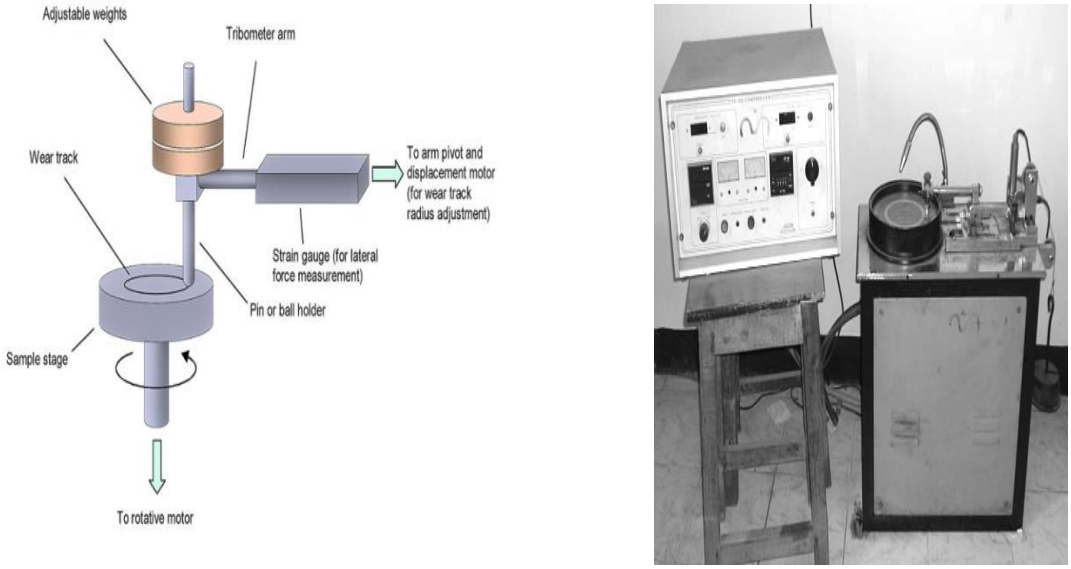

Figure 8. Sliding wear test apparatus

5 KN

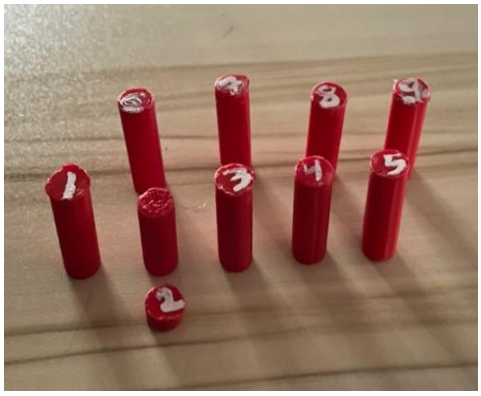

10 KN

15 KN

Figure 9. Wear samples

When applying several acceptable loads parallel to the specimen's axis, contact between the disc and the specimen must be created completely, and virgin material must be exposed to the disc, in order to get accurate and reproducible wear data. Table 4 lists the typical test parameters.

Table 4. Wear Test Conditions

Test parameter	Value	Unit
Load	5,10,15	N
Speed		m/s
Contact path diameter		mm
Test duration	10	Minutes
Lubricate	Dry	-
Room temperature	23 ± 2	°C
Humidity of the relative	50± 5	%
The envelope of gases surrounding the earth.	Air of the laboratory	-

The volume of wear (in cubic millimeters) is calculated by multiplying the cross sectional area by the height decrease, and the sliding distance (in meters) is calculated by dividing the time by the rotation speed. As a function of wear volume and sliding distance, wear statistics are presented.

Rate of wear = ΔW/DS …… (1)

ΔW :- test sites where large numbers of people were surveyed before and after an intervention (gm)

ΔW=W1-W2……..(2)

3. Results and discussion

Utilizing design of experiment, Taguchi method converts the response values into S/N ratio. Along with an assistance of (S/N) ratio, The best design with a fewest variations is possible. The current investigation's goal is to increase the specimens' mechanical characteristics. Therefore, greater was better when it came to qualities. The experimental results of the optimum levels for mechanical properties in S/N ratio are given shown in Tables 5, 6, and 7. The effect of printing speed has a rank (1) this mean have high effect between other processes. The print speed decreases with sufficient limit can improve the mechanical properties in general. Decreases printing speed at 50 mm/s will increases the wear properties. The results obtained indicate that increasing in printing speed reduces the impact strength. Low speed has been utilized, so that the material sticks well to the building plate on the first layer and this is one of the problems facing the work when utilizing printing speed at 100 mm/s. As the layer's thickness lowers, more layers become necessary, the distortion effect is reduced, and strength improves as a result. The layer's height also has a significant impact on the length of time needed for printing and the outcome of a smoother surface. The amount of layers needed to build an item impacts how quickly it can be printed and how long it will take to print. A 3D printed item of a given height takes longer to create the thinner the layer is. The number of cuts an item will get depends on the layer's thickness. Figures below demonstrate this (12 and 13), Decrease the layer's thickness to improve the layer's wear resistance. According to the results of wear tests, the optimal layer's thickness was 0.15 mm, while the 0.35 mm layer's thickness of specimens was not significant in specimens studied.Infill density included testing at 3 levels (30%, 60% and 90%). There is a great difference between 90% and 30% infill density for specimens. Thus, the ABS specimens are a stronger at 90% infill density. When the infill density of the specimens is high, around 90%, the mechanical characteristics are at their finest.

Table 5. Reaction Table of S/N ratios of wear rate at 5N

No. of Level	Printing Speed	The layer's thickness	Density of the Infill
L-1	0.00041	0.002574	0.000395
L-2	0.000456	0.000846	0.000764
L-3	0.002923	0.000846	0.002631
Deltas	**0.002513**	**0.002205**	**0.002236**
Ranking	**One**	**Three**	**Two**

Table 6. Reaction Table of S/N ratios of wear rate at 10N

No. of Level	Printing Speed	The layer's thickness	Density of the Infill
L-1	0.000549	0.001123	0.000544
L-2	0.000533	0.000738	0.000682
L-3	0.001226	0.000446	0.001082
Deltas	0.000292	0.000103	0.000390
Ranking	Two	Three	One

Table 7. Reaction Table of S/N ratios of wear rate at 15N

No. of Level	Printing Speed	The layer's thickness	Density of the Infill
L-1	0.000821	0.000774	0.000497
L-2	0.000805	0.000708	0.000769
L-3	0.000528	0.000672	0.000887
Deltas	0.000692	0.000677	0.000538
Ranking	One	Two	Three

In Tables 5, 6, and 7, the results obtained utilizing Taguchi method, as the following figures (10, 11, and 12) :

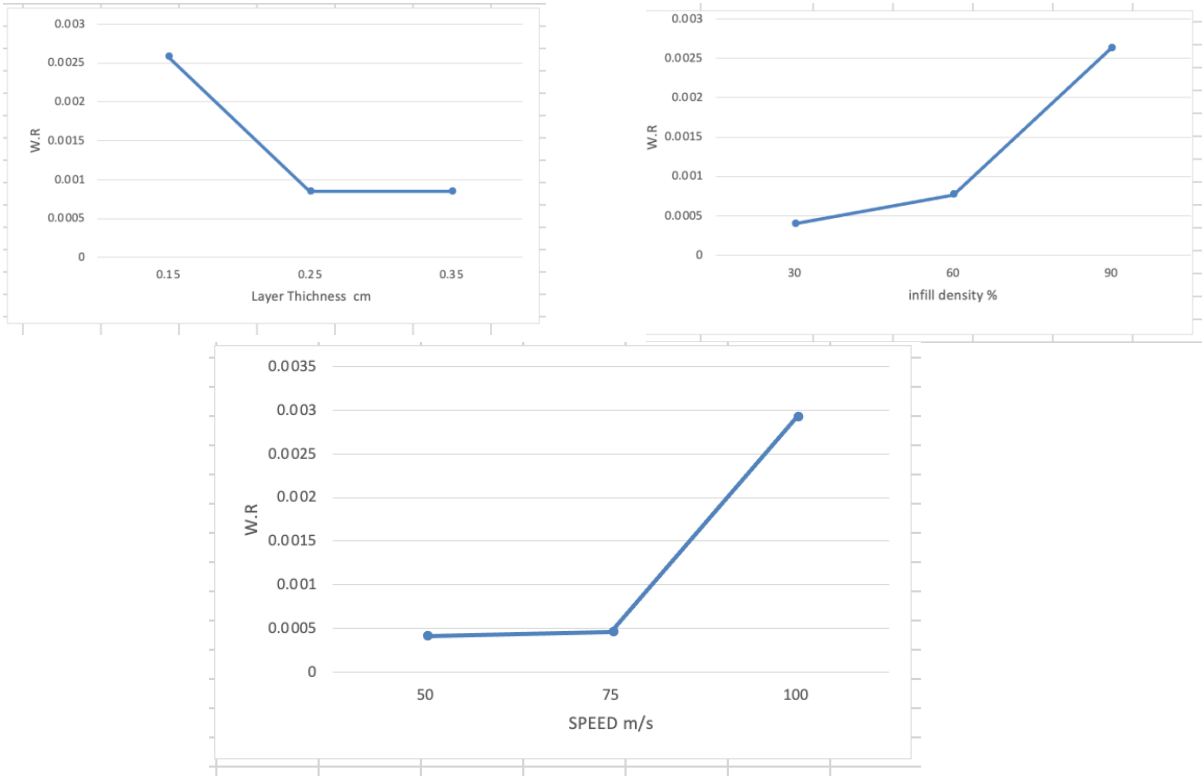

Figure 10. influence processing parameter on wear rate at 5N

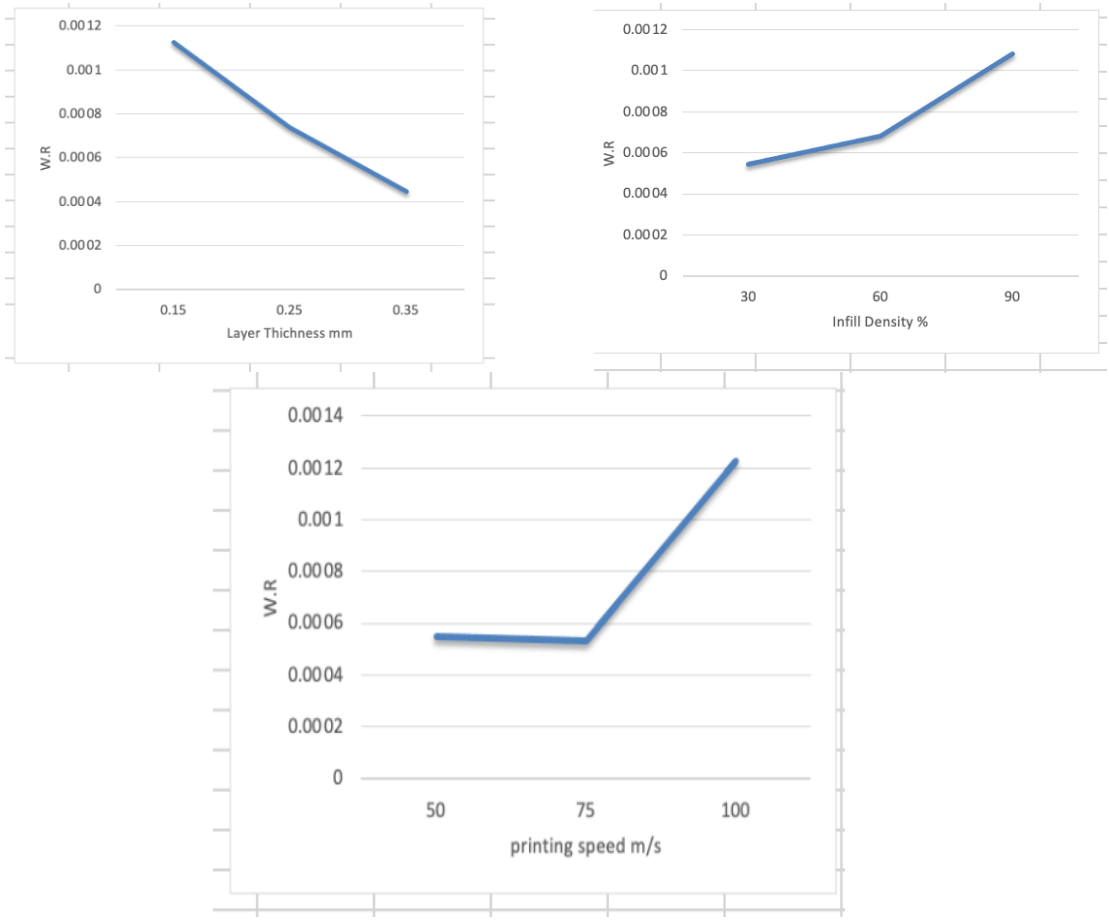

Figure 11. The influence processing parameter on wear rate at 10N

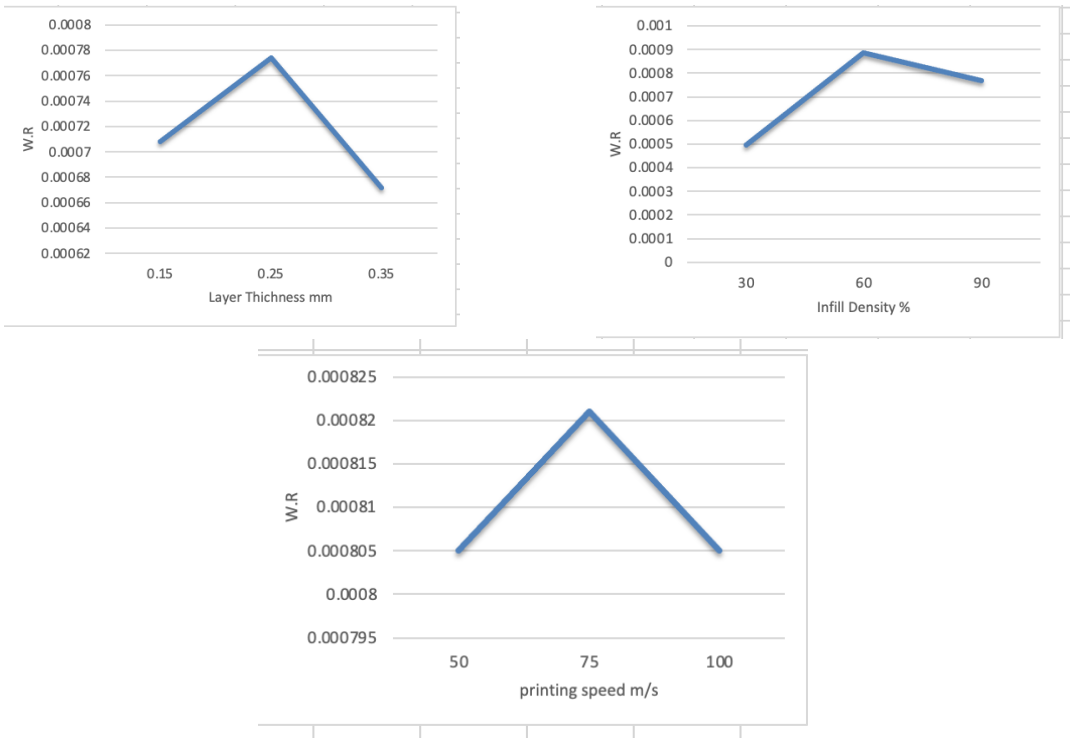

Figure 12. The influence processing parameter on wear rate at 15N

Abrasion and adhesion mechanisms cause the wear of polymers, which often begins with abrasion. By adjusting the applied stress for 5 minutes, the ABS material specimen shown extremely little material loss, as illustrated in Figure 10.

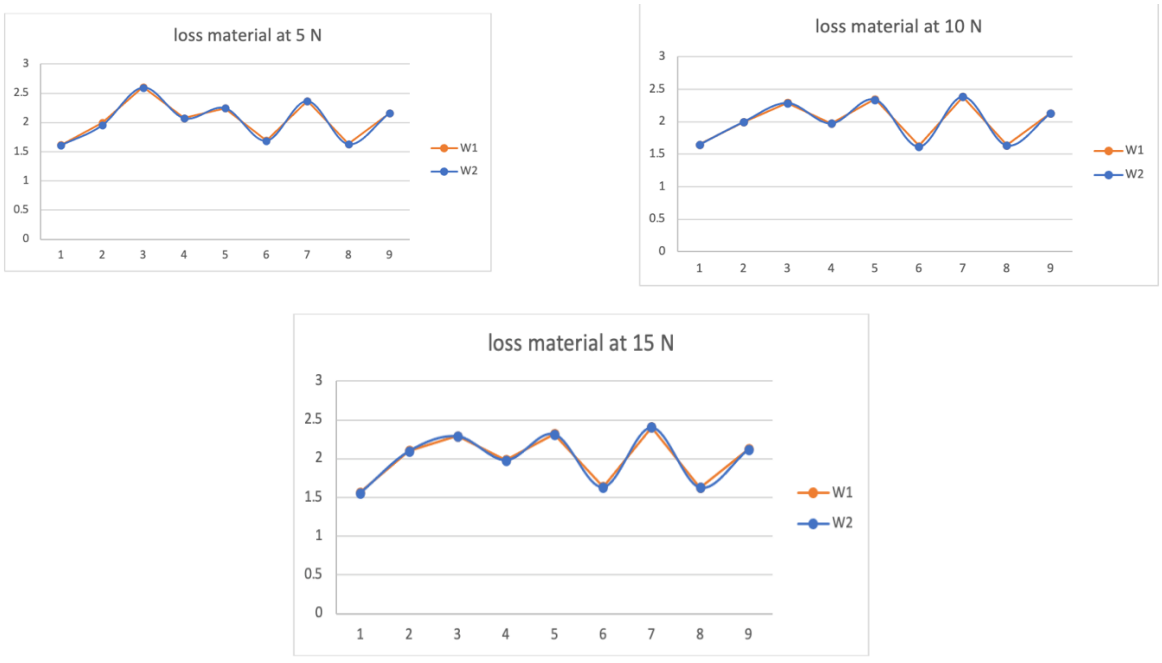

Figure 13. loss of material

The applied load determines the wear rate. Less wear loss occurs at lower applied load levels, whereas reinforced material breaks at higher applied loads. Significant material loss results from the separation of the material from the binder substance. As illustrated in Figures 14, 15, and 16, where the agglomeration rises with the load for

all the samples that were studied, some samples developed clumps and agglomerations as a result of the repetitive sliding movements of the sample on the abrasive surface.

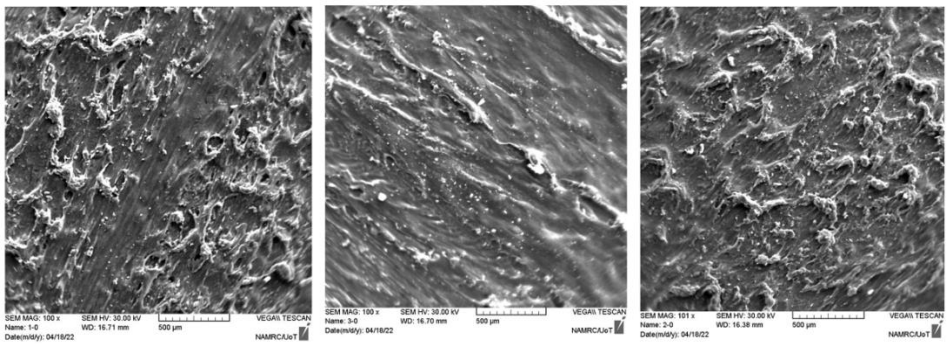

Figure 14. SEM images (500 µm)

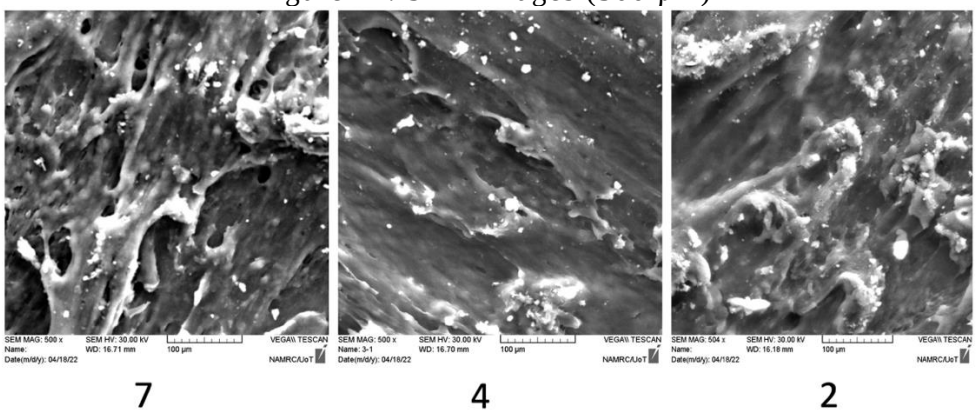

Figure 15. SEM images (100 µm)

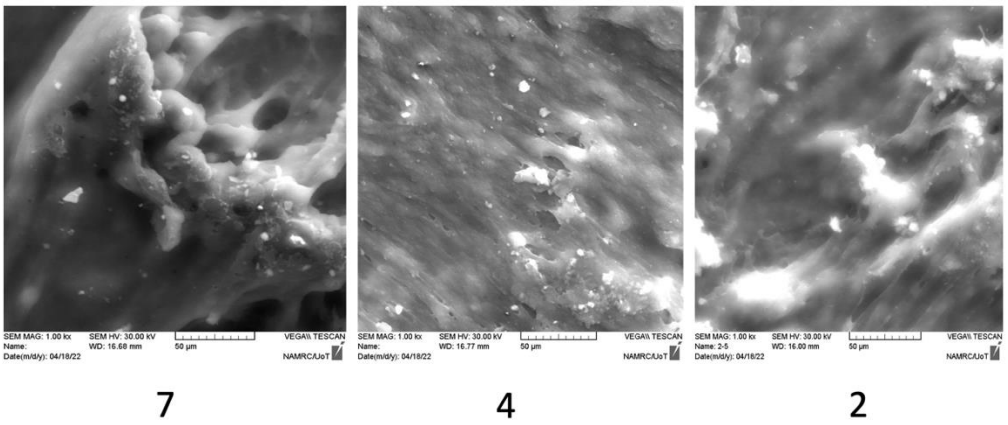

Figure 16. SEM images (50µm)

Abrasion is the first step in the wear process, and the specimen was cleaned of any debris left behind by wear when it was completed. When the load is raised, the ABS material will typically lose less volume than it will initially lose. Because of the rough, sliding surface that acts as an abrasive, the abrasive wear mechanism for the ABS material remains active during the entire test. The frictional push at the contact is increased by increasing the loading and operating duration, which accelerates the rate of wear. According to the calculations made utilizing Taguchi's method, sample No. 4 when the load is 5N, sample No. 2 when the load is 10N, and sample No. 4 when the load is 15N were found to be the best samples, and these samples are thought to be the best samples among the nine samples examined for each group. The reason for the appearance of lumps on the surface of the second sample is due to the the layer's thickness (0.35 mm), and the density of the filler was (60 percent) for the sample as it takes longer to build the sample as well as a longer time until the layers cooled and hardened, and this resulted in the appearance of lumps on the surface of the sample. This agglomeration may be due to the manufacturing conditions or factors utilized. The seventh sample's high filling density is the reason

why bumps started to appear on its surface. Figures 14, 15, and 16 show that adhesion and abrasion are the main wear mechanisms for plastic materials. The infill material wear tracks from the ABS material show that wear is cautilized through the transfer of a very thin layer of material at the point where two sliding surfaces come into touch with one another. A surface seems to be generally abrasion-free, clean, and lustrous. The specimen's defining characteristic, in addition to the evidence of abrasive wear, is that there seems to be very little surface delamination and plastic deformation.

4. Conclusions

Table displays the wear results of ABS samples created utilizing FDM. Utilizing a pin on the disk device, the impact of contact load (5N, 10N, and 15N) at constant rotation speed (950 rpm) and constant duration of 5 min at room temperature was studied. The ideal parameters for the ABS specimens in terms of wear rate were a speed of printing of 50 mm/s, the the layer's thickness of 0.25 mm, and a density of the infill material that was 60 percent of the total volume. Speed of the printing, the layer's thickness, and density of the infill are the three elements that are cited as having the most significant impact on wear rate. It should be noted that the wear characteristics of components created utilizing FDM are highly dependent on the process factors, and that these characteristics can be improved by carefully modifying the FDM parameter values. The crucial FDM parameters in the current study, including shell thickness (0.2mm), component orientation (0), infill pattern (gyroid), and nozzle diameter (0.6mm), were maintained throughout the project. Future research may concentrate on improving the aforementioned metrics on the test specimens' sliding wear.

Conflict of Interest

The authors declare that they have no conflict of interest, and all of the authors agree to publish this paper under academic ethics.

Author Contributions

All the authors contributed equally to the manuscript.

Funding information

This study did not obtain funding from any monetary institution.

References

[1] R. Hashemi Sanatgar, C. Campagne, and V. Nierstrasz, "Investigation of the adhesion properties of direct 3D printing of polymers and nanocomposites on textiles: Effect of FDM printing process parameters," *Applied Surface Science*, vol. 403, pp. 551-563, 2017, doi: 10.1016/j.apsusc.2017.01.112.

[2] S. R. Jason Cantrell1, David Damiani2, Rishi Gurnani3, Luke DiSandro1, Josh Anton1, Andie Young1, Alex Jerez1, Douglas Steinbach1, Calvin Kroese1, and Peter Ifju1, "Experimental Characterization of the Mechanical Properties of 3D-Printed ABS and Polycarbonate Parts," in *Conference Proceedings of the Society for Experimental Mechanics Series*, vol. 3, 2017.

[3] G. Gao, F. Xu, J. Xu, G. Tang, and Z. Liu, "A Survey of the Influence of Process Parameters on Mechanical Properties of Fused Deposition Modeling Parts," *Micromachines (Basel)*, vol. 13, no. 4, Mar 2022, doi: 10.3390/mi13040553.

[4] T. F. Abbas, A. Hind Basil, and K. K. Mansor, "Influence of Fdm Process Variables' on Tensile Strength, Weight, and Actual Printing Time When Using Abs Filament," *International Journal of Modern Manufacturing Technologies*, vol. 14, no. 1, pp. 7-13, 2022, doi: 10.54684/ijmmt.2022.14.1.7.

[5] S. H. Ahn, M. Montero, D. Odell, S. Roundy, and P. K. Wright, "Anisotropic material properties of fused deposition modeling ABS," *Rapid Prototyping Journal*, vol. 8, no. 4, pp. 248-257, 2002, doi: 10.1108/13552540210441166.

[6] A. Farzadi, M. Solati-Hashjin, M. Asadi-Eydivand, and N. A. Abu Osman, "Effect of layer thickness and printing orientation on mechanical properties and dimensional accuracy of 3D printed porous

samples for bone tissue engineering," *Plos One,* vol. 9, no. 9, pp1-16, 2014, doi: 10.1371/journal.pone.0108252.

[7] K. Singh Boparai, R. Singh, and H. Singh, "Wear behavior of FDM parts fabricated by composite material feed stock filament," *Rapid Prototyping Journal,* vol. 22, no. 2, pp. 350-357, 2016, doi: 10.1108/rpj-06-2014-0076.

[8] P. B. Patel, J. D. Patel, and K. D. Maniya, "Application of PSI Methods to Select FDM Process Parameter for Polylactic Acid," *Materials Today: Proceedings,* vol. 5, no. 2, pp. 4022-4028, 2018, doi: 10.1016/j.matpr.2017.11.662.

[9] R. Keshavamurthy, V. Tambrallimath, A. Badari, R. Krishna, G. S. Kumar, and M. C. Jeevan, "Friction and wear behaviour of copper reinforced acrylonitrile butadiene styrene based polymer composite developed by fused deposition modelling process," *FME Transactions,* vol. 48, no. 3, pp. 543-550, 2020, doi: 10.5937/fme2003543K.

[10] B. Ozcelik, A. Ozbay, and E. Demirbas, "Influence of injection parameters and mold materials on mechanical properties of ABS in plastic injection molding," *International Communications in Heat and Mass Transfer,* vol. 37, no. 9, pp. 1359-1365, 2010, doi: 10.1016/j.icheatmasstransfer.2010.07.001.

[11] O. H. Yahya, H. T. S. AlRikabi, R. M. Al_Airaji, and M. Faezipour, "Using internet of things application for disposing of solid waste," *International Journal of Interactive Mobile Technologies,* Article vol. 14, no. 3, pp. 4-18, 2020, doi: 10.3991/ijim.v14i13.13859.

[12] C.-P. Jiang, Y.-C. Cheng, H.-W. Lin, Y.-L. Chang, T. Pasang, and S.-Y. Lee, "Optimization of FDM 3D printing parameters for high strength PEEK using the Taguchi method and experimental validation," *Rapid Prototyping Journal,* vol. 28, no. 7, pp. 1260-1271, 2022, doi: 10.1108/RPJ-07-2021-0166.

[13] Sudin and et al., "Comparison of wear behavior of ABS and ABS composite parts fabricated via fused deposition modelling," *International Journal of ADVANCED AND APPLIED SCIENCES,* vol. 5, no. 1, pp. 164-169, 2018, doi: 10.21833/ijaas.2018.01.022.

[14] J. K. Oleiwi and R. A. Mohammed, "Comparison of the Wear Behavior and Hardness of Vinylester Resin Reinforced by Glass Fiber and Nano ZrO2 and Fe3O4," *Revue des composites et des matériaux avancés,* vol. 31, no. 6, pp. 325-333, 2021, doi: 10.18280/rcma.310603.

[15] A. Çoban, A. Demirer, and F. Ficici, "Optimization of Wear Parameters of Polyamide-6 Composite Materials Filled with Wollastonite Particles," *Periodicals of Engineering and Natural Sciences (PEN),* vol. 2, no. 1, 2014, doi: 10.21533/pen.v2i1.35.

[16] H. B. Ali, J. K. Oleiwi, and F. M. Othman, "Compressive and Tensile Properties of ABS Material as a Function of 3D Printing Process Parameters," *Revue des composites et des matériaux avancés,* vol. 32, no. 3, pp. 117-123, 2022, doi: 10.18280/rcma.320302.

[17] H. B. Ali and D. R. Alazawi, "Influence of layer bonding on compressive strength of 3D printed structure: An experimental study," *Sustainable Engineering and Innovation,* vol. 4, no. 1, pp. 76-81, 2022, doi: 10.37868/sei.v4i1.id159.

[18] J. Mago, R. Kumar, R. Agrawal, A. Singh, and V. Srivastava, "Modeling of Linear Shrinkage in PLA Parts Fabricated by 3D Printing Using TOPSIS Method," in *Advances in Additive Manufacturing and Joining,* (Lecture Notes on Multidisciplinary Industrial Engineering, 2020, ch. Chapter 23, pp. 267-276.

[19] M. Z. M. H. amli R., Lim K. C.,Yusoff Y. and Yusuff M. S., "INTERACTION TESTING FOR AN AD-HOC SYSTEM (QUEUEMANAGEMENT SYSTEM)," *ARPN Journal of Engineering and Applied Sciences,* vol. 10, no. 3, pp. 1161-1168, 2015.

[20] D. R. A. H.B. Ali "Characterization of fatigue properties of 3D printed polylactic acid," *Periodicals of Engineering and Natural Sciences,* vol. 10, no. 3, pp. 334-340, 2022.

[21] O. S. Es-Said, J. Foyos, R. Noorani, M. Mendelson, R. Marloth, and B. A. Pregger, "Effect of Layer Orientation on Mechanical Properties of Rapid Prototyped Samples," *Materials and Manufacturing Processes,* vol. 15, no. 1, pp. 107-122, 2000, doi: 10.1080/10426910008912976.

[22] R. H. Abdel-Rahim, M. S. Attallah, and R. A. Mohammed, "Investigation the Effect of Nano Silica Dioxide Additives on the Properties of Epoxy Resin for Using in Industrial Applications," *Materials Science Forum*, vol. 1050, pp. 103-113, 2022.

[23] V. H. Panchakshari, K. M. Ravichandra, M. Kotresh, and N. Ranganath, "Optimization of process parameters of cryogenic treatment on Al/Al2O3 MMCs by Taguchi method for tensile strength," *Periodicals of Engineering and Natural Sciences (PEN)*, vol. 6, no. 2, 2018, doi: 10.21533/pen.v6i2.267.

[24] B. Durakovic, "Design for additive manufacturing: Benefits, trends and challenges," *Periodicals of Engineering and Natural Sciences (PEN)*, vol. 6, no. 2, 2018, doi: 10.21533/pen.v6i2.224.

[25] H. Unal and F. Findik, "Friction and wear behaviours of some industrial polyamides against different polymer counterparts under dry conditions," *Industrial Lubrication and Tribology*, vol. 60, no. 4, pp. 195-200, 2008, doi: 10.1108/00368790810881542.